J Inorg Organomet Polym (2016) 26:788–798
DOI 10.1007/s10904-016-0387-6

Investigation of Characterization and Mechanical Performances of Al_2O_3 and SiC Reinforced PA6 Hybrid Composites

S. Sathees Kumar[1] · **G. Kanagaraj**[2]

Received: 11 February 2016 / Accepted: 14 May 2016 / Published online: 6 June 2016

Abstract In this study, the influence of different weight percentages of alumina oxide (Al_2O_3) and silicon carbide (SiC) reinforcement on the mechanical properties of Polyamide (PA6) composite is investigated. Test specimens of pure PA6, 85 wt% PA6 + 10 wt% Al_2O_3 + 5 wt% SiC and 85 wt% PA6 +10 wt% SiC + 5 wt% Al_2O_3 are prepared using an injection molding machine. To investigate the mechanical behaviors tensile test, impact test, flexural test, and hardness test were conducted in accordance with ASTM standards. Experimental results indicated that the mechanical properties, such as tensile, impact, hardness, and flexural strength were considerably higher than the pure PA6. The tensile fracture morphology and the characterization of PA6 hybrid composites were observed by scanning electron microscope and Fourier transform infrared spectroscopic method. Further, thermogravimetric analysis confirms the thermal stability of PA6 hybrid composites. The reinforcing effects of Al_2O_3 and SiC on the mechanical properties of PA6 hybrid composites were compared and interpreted in this paper. Improved mechanical and thermal characteristics were observed by the addition of small amount of Al_2O_3 and SiC simultaneously reinforced with the pure PA6.

✉ S. Sathees Kumar
shrutishyami@gmail.com

G. Kanagaraj
gkmech@tce.edu

[1] Department of Mechanical Engineering, Latha Mathavan Engineering College, Madurai, Tamil Nadu 625301, India

[2] Department of Mechanical Engineering, Thiagarajar College of Engineering, Madurai, Tamil Nadu 625015, India

Keywords Polyamide · Al_2O_3 · SiC · Hybrid composites · Mechanical Properties

1 Introduction

In recent years, polymeric material gained significant importance in engineering field due to its light weight, environmental resistance and helpful mechanical properties such as specific strength, toughness, and excellent abrasion resistance [1]. Polyamide (PA6) is a high-performance engineering plastic used in electrical/electronics, automobile, packaging, textiles and consumer applications because of its excellent mechanical properties [2]. However, limitations in mechanical property's level, the low heat deflection temperature, high water absorption and dimensional instability of pure PA6 have prevented its wide range of applications. To overcome this difficulty, many researchers paid attention and improved the property of PA6 significantly by reinforcement methods. Reinforcements are usually done to improve the properties of the base metals like strength, stiffness, conductivity, etc. The mechanical and tribological behavior of polyamide, high-density polyethylene (HDPE), and their composites have been studied and reported in the literature [3, 4]. For further improvement of polymer materials, some research works are carried out by polyamide materials reinforced with polymers, metals, and ceramics.

Palabiyik and Bahadur [5] investigated the mechanical and tribological properties of PA6 and HDPE, polyblends with and without the compatibilizing agent maleicanhydride propylene, and they observed that the best coefficient of friction and high wear resistance was identified in the composites consisting 40 % of PA6 and 60 % of HDPE and 80 % of PA6 and 20 % of HDPE, respectively, by weight.

Bose and Mahanwar [6] studied the effects of adding mica with variable particle size on the mechanical, thermal, electrical and rheological properties of nylon-6. Composites of nylon-6 with varying concentrations (viz. 5 to 40 wt %) of mica were prepared by twin screw extrusion. They observed that a mechanical and electrical properties increases with decrease in particle size. Shi et al. [7] examined the impact fracture behaviors of polyamide 6 (PA6) composites with tetra-needle-shaped zinc oxide whisker (T-ZnOw). They compared with the composites filled with untreated T-ZnOw, in which the impact strength decreases linearly with the increasing content of filler, chemically treated T-ZnOw improves the impact strength of the composites apparently due to the improved interfacial interaction between T-ZnOw and matrix.

Ularych et al. [8] studied the dependence of the mechanical properties of the length of reinforcing fibers in hydrolytic PA6 matrix. Modulus, tensile strength, and also impact strength measured on test pieces seem to be a linear function of the part of fiber length population (percentile) representing the reinforcing fibers longer than 200 μm. Tang et al. [9] inspected the mechanical properties of carbon fiber reinforced composites and PA6 particles dispersed carbon fiber hybrid-reinforced composites. They found that the mechanical properties were improved by incorporating PA6 particles into the polytetrafluoroethylene (PTFE) matrix and the hybridization of the fiber-reinforced PTFE composites by PA6 fillers showed the improvement of mechanical properties. The Polyamide 6 composites filled with up to 30 wt% spherical glass beads, and flake-like talc fillers, were prepared by extrusion and injection moulding [10].

Zhang et al. [11] examined the microstructure and mechanical properties of reaction bonded SiC reinforced with random chopped carbon fibers of 3 mm length. The composites were fabricated by dispersing chopped carbon fibers into bimodal SiC/C suspension, forming green body through slip casting, and then reaction sintering at 1700 °C. The effect of the chopped fiber fraction on microstructure and mechanical properties was evaluated. A significant increase of fracture toughness was obtained as the carbon fiber fraction approaches 30 vol%. The epoxy nanocomposites, prepared using a synthesized hybrid carbon nanotube–alumina (CNT–Al_2O_3) filler, via chemical vapour deposition and a physically mixed CNT–Al_2O_3 filler, at various filler loadings (i.e., 1–5 %) by [12]. The tensile and thermal properties of both nanocomposites were investigated at different weight percentages of filler loading. They demonstrated that the CNT–Al_2O_3 hybrid epoxy composites are capable of increasing tensile strength by up to 30 %, giving a tensile modulus of 39 %, thermal conductivity of 20 %, and a glass transition temperature value of 25 % when compared to a neat epoxy composite.

The effects of basalt fibre (BF) and montmorillonite (MMT) co-reinforced polyamide 6 (PA6) matrix hybrid nanocomposites were prepared by injection moulding and their mechanical properties were investigated in [13]. From the results they viewed that the hybrid nanocomposites revealed high tensile and flexural properties, and a synergistic effect of the co-reinforcement has been demonstrated. They observed that the presence of short BF can enhance the dispersion of the nanoparticles in the matrix. The effects of zeolite particles on the mechanical and tribological properties of the ultra-high molecular weight polyethylene (UHMWPE) composites were studied by Boon et al. [14]. They observed that the 10 wt% zeolite/UHMWPE composites showed an increase of 25 % in impact strength as compared to pure UHMWPE. The 20 wt % zeolite/UHMWPE composite exhibited lowest wear volume loss as compared to 10 wt% zeolite/UHMWPE and pure UHMWPE. Amal Nassar and Eman Nassar [15] studied the effect of Nano SiC particles on the mechanical properties of the epoxy polymer composite material. They found that the addition of SiC nanoparticles to epoxy cause a drop in the strength of the alloy at room temperature continuously as the SiC nanoparticles increase from 10 to 20 wt% as the strength decreases with further increase in the weight percentage of the reinforcement.

Recently, Sathees Kumar and Kanagaraj [16] experimentally studied the mechanical properties of Al_2O_3 reinforced PA6 composites with varying weight percent of Al_2O_3 (5, 10, 20 and 30 %). They found that the enhanced mechanical properties of tensile and flexural strength obtained in 90 wt% PA6 + 10 wt% Al_2O_3 composites. Further, they investigated [17] the mechanical properties of SiC reinforced PA6 composites with varying weight percent of SiC (5, 10, 20 and 30 %). The results revealed that the mechanical properties of tensile and hardness were improved in 10 wt% SiC + 90 wt% PA6 composites. From the aforementioned research works, it can be concluded that Al_2O_3 and SiC has been widely used as filler material with PA6 to increase high strength, low thermal expansion, high thermal conductivity, high hardness, high elastic modulus and excellent thermal shock resistance.

To the best of our knowledge, the combined effects of Al_2O_3 and SiC reinforced PA6 composites on mechanical behaviors have not been published. In this study, the combined reinforcing effects of Al_2O_3 and SiC on the mechanical properties of PA6 hybrid composites were investigated. The test specimen of pure PA6, 85 wt% PA6 + 10 wt% Al_2O_3 + 5 wt% SiC and 85 wt% PA6 +10 wt% SiC + 5 wt% Al_2O_3 were prepared using an injection molding machine. The mechanical properties were evaluated by conducting tensile, impact and hardness test. The tensile fracture morphology and the characterization of PA6 hybrid composites were observed by scanning

electron microscope (SEM) and Fourier transform infrared (FT-IR) spectroscopic method. Additionally, thermogravimetric analysis (TGA) conducted on PA6 hybrid composites to analyze its thermal stability.

2 Experimental Details

2.1 Chemicals and Instrumentation

The density and the melting temperature for Polyamide 6 (PA6) are 1.14 g/cm^3 and 220 °C respectively. PA6 is purchased as pellets of size 3 mm. SiC purchased as 200 mesh with a particle size of 2 microns and Al_2O_3 with the particle size of 150 mesh, 88 micron, and 0.0035 inches. Both particles were supplied by Modern Scientific Co., Ltd., Madurai, Tamil Nadu, India. The test specimens are prepared using an injection molding machine with maximum chamber capacity of 150 g. The muffle furnace is supplied by Prabha machine tools, Coimbatore, Tamil Nadu, India. The tensile test was conducted on a Tinius Olsen UTM 10 kN Electronic testing machine. The impact test was conducted on a Tinius Olsen tester and the hardness test was conducted on a Shore D hardness test machine (Model—SRT-102) supplied by S. C. Dey & Co. Kolkata, India.

2.2 Preparation Process of Test Specimen

In order to evaluate the mechanical properties of PA6 blended with alumina and SiC, the blends are produced in different proportions of 5 and 10 % by weight of each particle. The injection molding machine is maintained at the temperature of 190 °C. The resistance temperature detector (RTD) sensor is inserted in the circumference of the injection molding machine for temperature measurement. The moulding dies are preheated up to 75 °C for free flow of melted materials. In the first stage, Al_2O_3/SiC are preheated in muffle furnace. The preheating processes temperature of 1800 °C for SiC and 1950 °C for Al_2O_3. After reaching the temperature of 1800 °C for preheated SiC and 1950 °C for preheated Al_2O_3 are cooled at atmospheric temperature in 45 min. Then preheated Al_2O_3 and SiC are added with PA6 and stirred. The blended PA6/Al_2O_3/SiC composite materials are put into injection moulding machine to make test specimen. Figure 1 shows the schematic diagram of preparation process of test specimen using an injection molding machine. The details of composites prepared for the present study are listed in Table 1.

The test specimen dimensions for tensile test, impact test, hardness test and flexural test are 115 × 20 × 3 mm according to ASTM D638, 63.5 × 12.7 × 3.2 mm according to ASTM D256, 35 × 15 × 3 mm according to ASTM D2240, 110 × 15 × 3 mm according to ASTM D790, respectively shown in diagrammatically in Fig. 2a–d. The properties of PA6, Al_2O_3 and SiC are listed in Table 2.

2.3 Mechanical Tests

2.3.1 Tensile Test

Tensile properties such as tensile strength, percentage elongation at break and tensile modulus were measured using microprocessor controlled universal testing machine (UTM) with an accuracy of ±2 MPa in accordance with the ASTM D638-01 standard at cross head speed of 5 mm/min and a gauge length of 75 mm. At least minimum of five samples of each specimen was tested at room temperature for each composition and an average value was taken for analysis. Tensile modulus and tensile strength are evaluated from the load-displacement curve.

2.3.2 Flexural Test

Flexural properties such as flexural strength and flexural modulus test were performed as per ASTM D790 standard using the UTM (Tinius Olsen UTM, capacity 1–10 kN). For the flexural test, a three-point bending configuration was selected with a support span length of 70 mm. The cross-head speed of the machine was set at 2 mm/min. The measurements were taken at five magnitudes of the constant load for five specimens.

2.3.3 Impact (Izod) Test

The impact test is conducted on a Tinius Olsen testing machine according to ASTM D256 standard. Izod specimens are unnotched to prevent deformation of the specimen upon impact. This test can be used as a quick and easy quality control check to determine if a material meets specific impact properties or to compare materials for general toughness. This test involves the sudden and dynamic application of the load on the specimen. This test measures the amount of energy absorbed by the specimen for the break in kJ/m^2.

2.3.4 Hardness Test

The ASTM D2240 standard specimen was used for hardness test in shore (Durometer) hardness tester (Make—Hiroshima) 1.40 mm diameter 30º Cone indentor extension up to 2.54 mm with an applied force of 44.45 N. The test specimens were kept under the indenter of shore D testers and the deflection on the scale was noted. The indentation

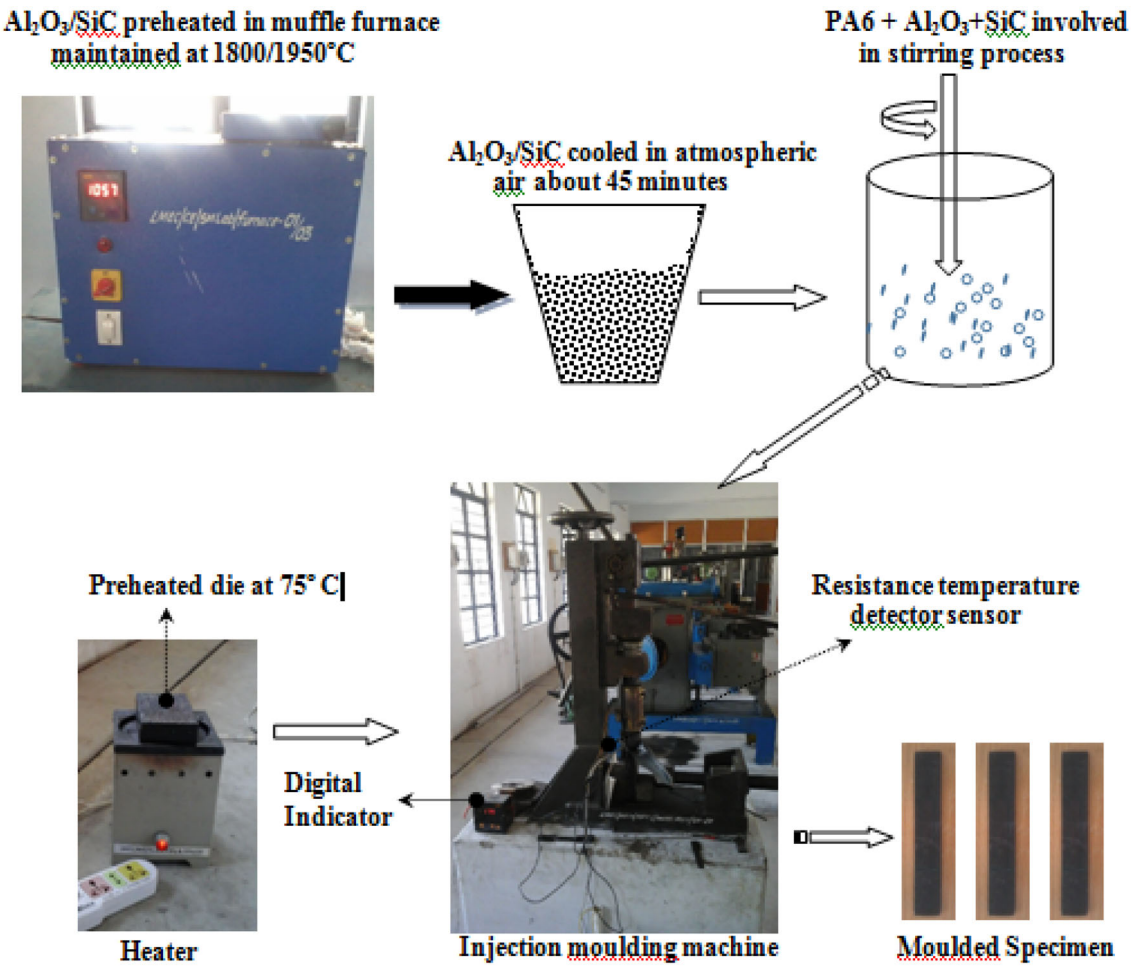

Fig. 1 Preparation process of Al_2O_3 and SiC reinforced PA6 test specimen

Table 1 Composites prepared for the present study

Sample name	PA6 (wt%)	Al_2O_3 (wt%)	SiC (wt%)
Specimen-1	100	–	–
Specimen-2	85	5	10
Specimen-3	85	10	5

value reflects the resistance to local deformation, which is a complex property and related to modulus, strength, elasticity, plasticity and dimensional stability. It also gives an idea about the degree of cross linking. A minimum of six readings was noted down for each sample at different positions and an average value was recorded.

3 Results and Discussion

3.1 Mechanical Properties of PA6 Hybrid Composites

Figures 3 and 4 shows the variation of tensile strength, tensile modulus for the PA6 and Al_2O_3/SiC/PA6 composites. It is clear from Figs. 3 and 4 that the addition of Al_2O_3 and SiC with pure PA6 can increase tensile strength and tensile modulus slightly. Tensile strength of specimen 3 was improved up to 18.1 % compared with specimen 1. This is because of uniform dispersion of Al_2O_3 and SiC with pure PA6. Again there is a reduction in the elongation at break of the composites with an increase in the weight fraction of Al_2O_3 (Fig. 5). This is due to the fact that the Al_2O_3 filler is hard and also highly brittle. As the small wt% of Al_2O_3 increase, the tensile modulus of PA6 composites increases, but at the same time, the resultant composites becomes more brittle. Uniform dispersion and the better interfacial adhesion between the dispersed phase and the matrix are the important factors that dominate the tensile properties of the composites [20]. It clearly reveals that the major addition Al_2O_3 in specimen 3 was enhanced the ductile property of PA6. Figure 5 shows the variation of break load, maximum displacement and percentage elongation of all specimens. Specimen 3 has the highest value of maximum displacement and break load. Percentage of elongation has highest at specimen 1 followed by specimen

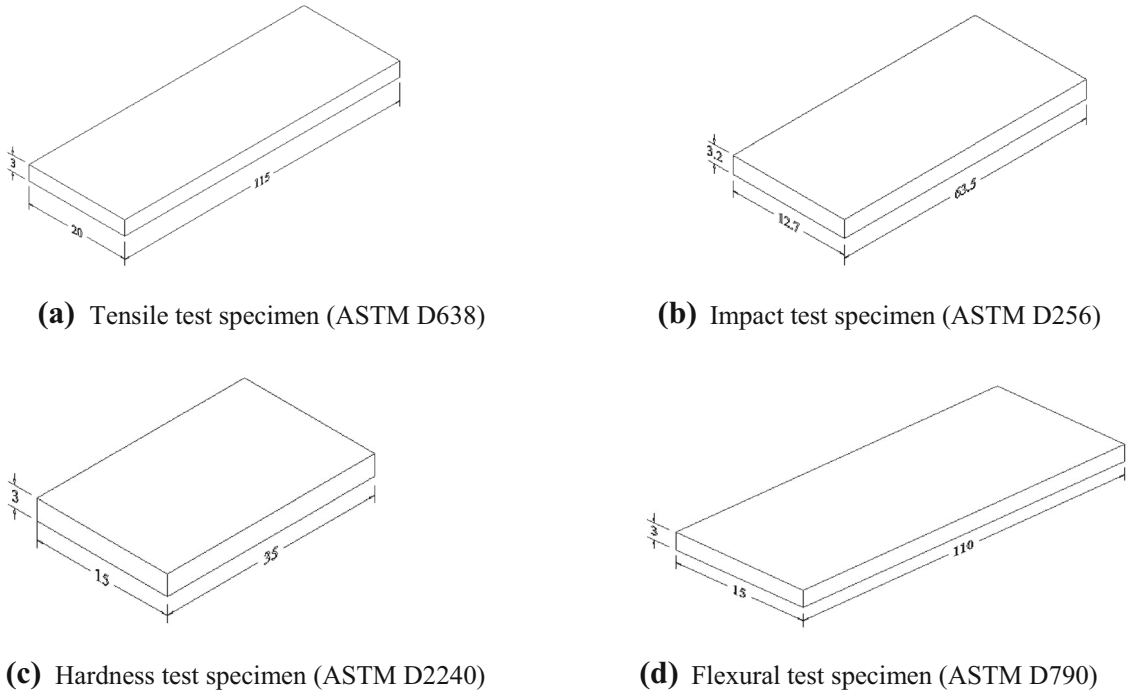

(a) Tensile test specimen (ASTM D638)

(b) Impact test specimen (ASTM D256)

(c) Hardness test specimen (ASTM D2240)

(d) Flexural test specimen (ASTM D790)

Fig. 2 Dimensions of test specimen used in the study. **a** Tensile test specimen (ASTM D638). **b** Impact test specimen (ASTM D256). **c** Hardness test specimen (ASTM D2240). **d** Flexural test specimen (ASTM D790)

Table 2 Properties of PA6, Al_2O_3 and SiC

Materials	Tensile strength (MPa)	Tensile Modulus (MPa)	Thermal conductivity (w/m°K)	Hardness	References
PA6	80	3000	0.245	82 (Shore -D)	[21]
Al_2O_3	260	300×10^3	30	14710–16180 (MPa)	[19]
SiC	135	350×10^3	120	VHN—20–30 (GPa)	[18]

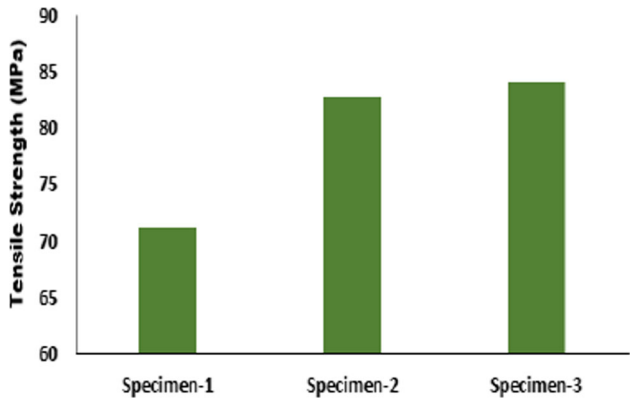

Fig. 3 Variation of tensile strength for PA6 composites

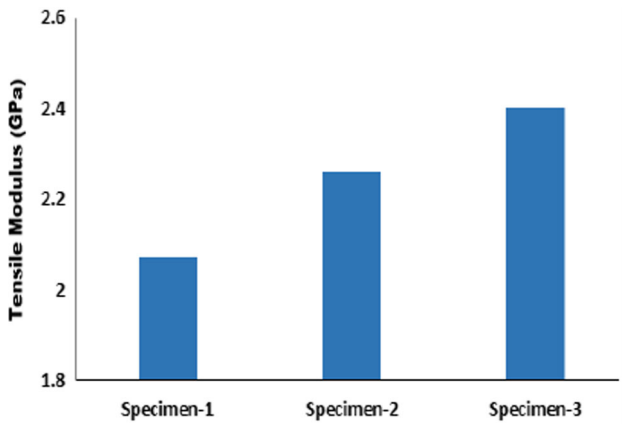

Fig. 4 Variation of tensile modulus for PA6 composites

3 and specimen 2. Break load of specimen 2 slightly low when compared with specimen 3 (Fig. 5). Similarly, the maximum displacement value was observed by specimen 3 than compared with both specimens 1 and 2. Figure 6 shows the flexural strength for the PA6 and Al_2O_3/SiC/PA6 composites. It can be noted that specimen 3 has the highest

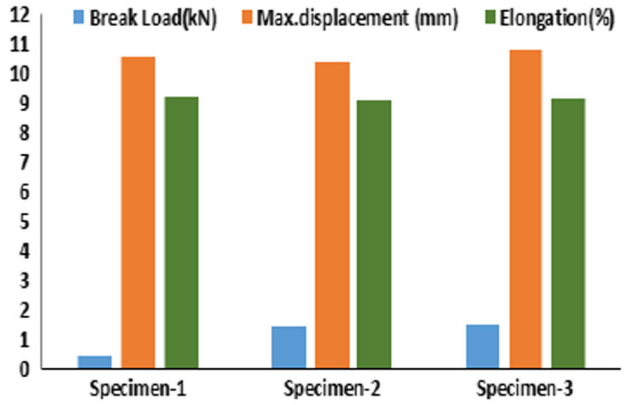

Fig. 5 Variation of break load, maximum displacement and elongation for PA6 composites

value of flexural strength followed by specimen 2 and specimen 1. The tensile strength of specimen 3 was improved up to 5 % compared with specimen 1.

Figure 7 shows the variation of flexural modulus of all specimens. Specimen 3 has the highest value of flexural modulus. Flexural modulus has highest at specimen 3 followed by specimen 2 and specimen 1. It was shown that the flexural strength and flexural modulus are improved obviously with the addition of SiC/Al_2O_3 in the PA6 composites. The incorporation of both SiC and Al_2O_3 significantly increased the flexural strength and flexural modulus of PA6. Compared with the specimen 1 and specimen 2 composite, the flexural modulus and flexural strength of specimen 3 was higher because of the strong interaction and interfacial adhesion between the polymer molecules chains. Specimen 2 has the marginally lower value of flexural strength and flexural modulus properties when compared with specimen 3. It is clearly obvious that the addition of contents 5 wt% Al_2O_3 and 10 wt% SiC developed the composite specimen-2 turns into an inelastic property. An increase in the concentration of SiC particles

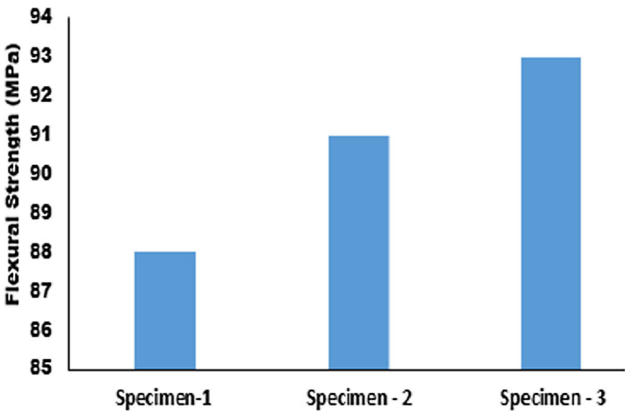

Fig. 6 Variation of flexural strength for PA6 composites

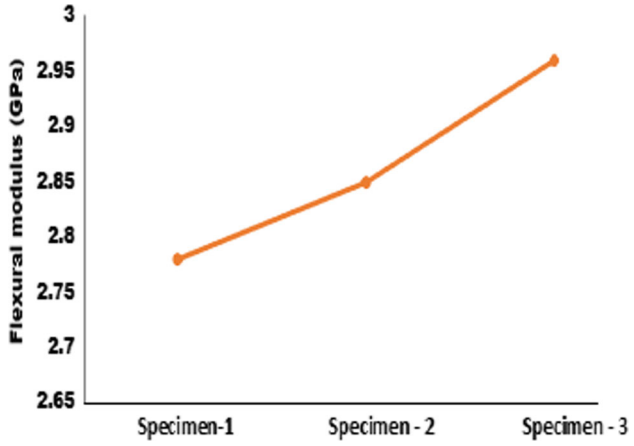

Fig. 7 Variation of flexural modulus for PA6 composites

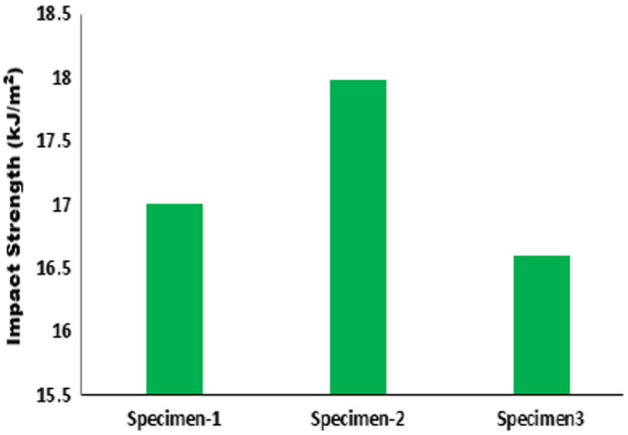

Fig. 8 Variation of impact strength for PA6 composites

increases the ability of the matrix to absorb hardness and thereby reducing the flexural strength and flexural modulus. Specimen 3 has the highest value of flexural strength and flexural modulus properties when compared with specimen 2 and specimen 1. It is clearly evident that the addition of 10 wt% Al_2O_3 and 5 wt% SiC shows the good ductile properties. The stiff nature of PA6 polymer was decreased with the addition of 10 wt% Al_2O_3 and 5 wt% SiC. The flexural property of Al_2O_3 is higher when compared with SiC. It clearly reveals that the major addition Al_2O_3 in specimen 3 was enhanced the yielding property of PA6.

Figure 8 shows the variation of impact strength of the all specimens. Specimen 2 has better impact strength followed by specimen 1 and specimen 3. It is seen that impact strength was improved evidently with the addition of SiC/Al_2O_3 in the PA6 composites. The lowest value was observed in specimen 3. The impact strength of specimen 2 was improved up to 5.76 % compared with specimen 1. It was observed that the impact strength of the specimen 2

was increased with content (5 wt% Al_2O_3 and 10 wt% SiC) in PA6 matrix. At high percentages of SiC and the low percentage of Al_2O_3 content were found to fine agree with the experimental results. Figure 9 shows the results of the hardness values of all specimens. SiC/Al_2O_3 contents added to the base polymer (PA6) that increases the hardness apparently. The high hardness containing specimen 3 is followed by specimen 2 and specimen 1. The smallest value is performed by specimen 1. The hardness value of specimen 3 (81.8) is 3.4 higher than the specimen 1 (78.4). The high hardness and thus the resistance undergo deformation have a mixture containing 5 wt% SiC and 10 % Al_2O_3 (specimen-3). It was observed that 10 wt% of Al_2O_3 and 5 wt%. SiC particles in the polymer matrix and hardness values of the PA6 composites have been increased. On the other hand, it can be suggested from the hardness test, the elastic behavior of the matrix proportionately varies with the addition of PA6 with 5 wt% Al_2O_3 and 10 % SiC particles (specimen-2). In summary, up to 10 wt% Al_2O_3 contents added to the base polymer (PA6) which increases the hardness apparently. The physico-mechanical properties of PA6 and PA6 composite test specimen obtained from the mechanical investigation are listed in Table 3.

From Table 3, it is well worth noting that the simultaneous addition of Al_2O_3 and SiC with PA6 can effectively improve the mechanical behavior of pure PA6 owing to the synergistic effects between them. Specimen 3 exhibited excellent mechanical property when compared with specimen 2. The fractured images of test specimens as shown in Fig.10a and b.

3.2 SEM Observation of Fracture Surface of the PA6 Composites

SEM is utilized to observed the tensile fracture surface of the pure PA6 and PA6 hybrid composites are represented

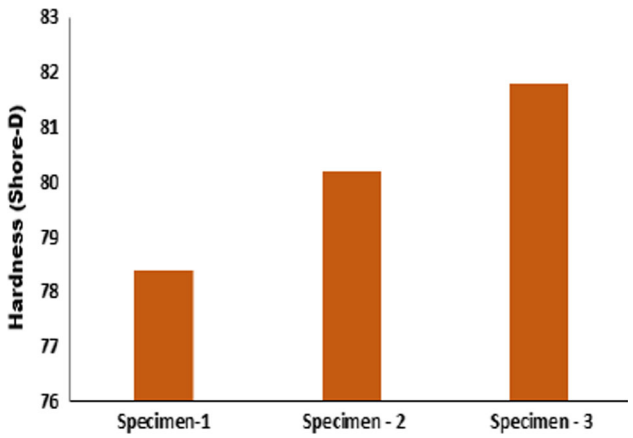

Fig. 9 Variation of hardness (Shore-D) for PA6 composites

Table 3 Physico-mechanical properties of tested PA6 and PA6 composite specimens

Properties	Specimen-1	Specimen-2	Specimen-3
Break load (kN)	0.44	1.45	1.52
Max.displacement (mm)	10.58	10.4	10.72
Tensile strength (MPa)	71.21	82.7	84.1
Elongation (%)	9.2	9.13	9.18
Tensile modulus (GPa)	2.07	2.26	2.4
Flexural strength (MPa)	88	91	93
Flexural modulus (GPA)	2.78	2.85	2.96
Impact strength (kJ/m^2)	17	17.98	16.6
Hardness (Shore-D)	78.4	80.2	81.8

in Fig. 11a–c. Figure 11a reveals the fracture surface of pure PA6 (specimen 1). It is clearly observed that severe plastic deformation and some broken particles occur on the surface due to the absence of Al_2O_3/SiC reinforcement. Figure 11b shows the fracture mechanism of specimen-2 (PA6—85 %, Al_2O_3—5 % and SiC—10 %). The general arrangement of the PA6/Al_2O_3/SiC is slightly visible in the image. The darker particles are SiC, white particles are Al_2O_3 and lighter ones are PA6. Here, the filler material dislocated due to poor interlinking.

The improper interlinking of Al_2O_3/SiC created voids, plastic deformation and broken particles on PA6 are followed. It is clearly visible that the fractured surface possesses some plastic deformation and the broken particles. This may be because of the addition of 10 wt% SiC and 5 wt%. Al_2O_3 takes place in a brittle way and agrees with the lowest elongation. On the other hand, inhomogeneity may occur by increasing the micro size particles such as SiC (10 wt%). The particles were poorly bonded to

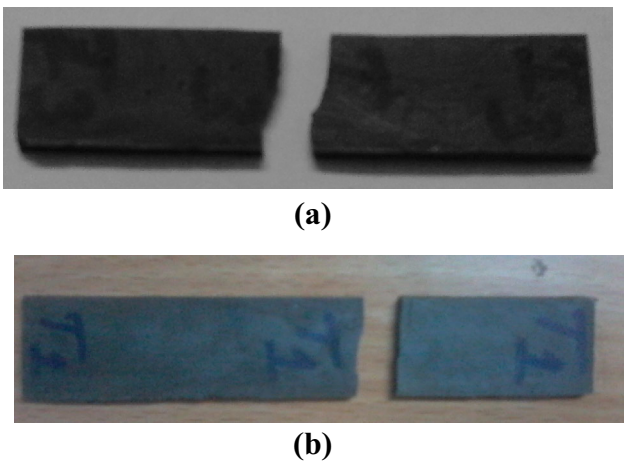

Fig. 10 Fractured images of test specimen. **a** Fractured impact test specimen. **b** Fractured tensile test specimen

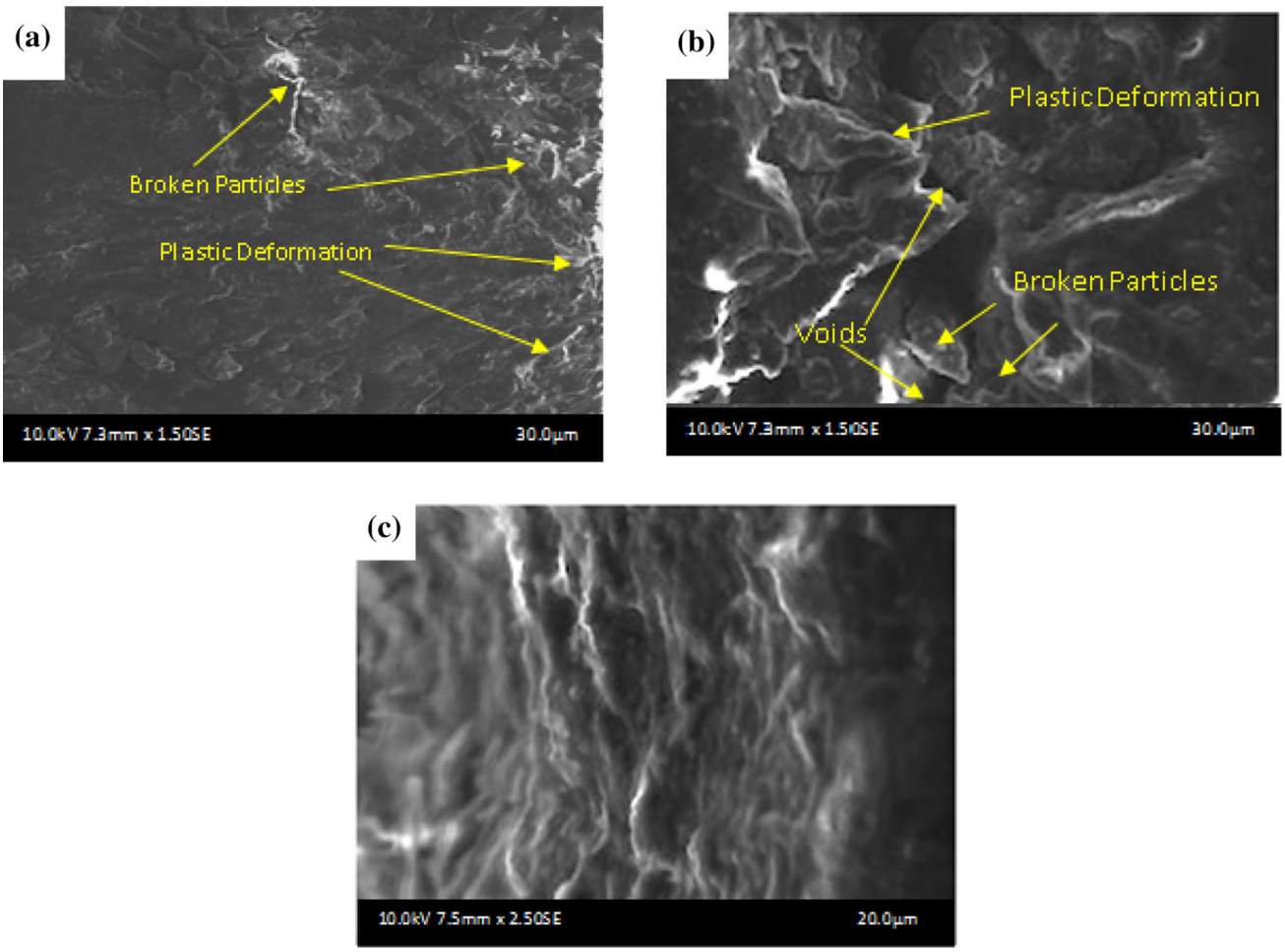

Fig. 11 SEM images of the fractured surfaces. **a** Specimen 1 (PA6—100 %). **b** Specimen 2 (85 wt% PA6 + 5 wt% Al_2O_3 + 10 wt% SiC). **c** Specimen 3 (85 wt% PA6 + 10 wt% Al_2O_3 + 5 wt% SiC)

the polymer matrix and split easily during the tensile test process. This absence of particle matrix linkage implied that the particles were incapable to crack trapping and thus could not help improvements in the tensile test. Moreover, the poorly bonded Al_2O_3/SiC particles acted as defects in the polymer material, thereby lowering the resistance to crack growth and thus leading to weakening in the tensile strength (Fig. 11b). The addition of SiC revealed negative effect on tensile properties of PA6 polymer composites; this fact was found back to inhomogeneity, plastic deformation and numerous voids and plastic deformation in the matrix.

Figure 11c shows the fracture mechanism of specimen-3 (PA6—85 %, Al_2O_3—10 % and SiC—5 %). The general arrangement of the PA6/Al_2O_3/SiC is clearly visible in the image. It shows that the uniform dispersion of Al_2O_3 and SiC particles with PA6 are compared with the other two images. It is clearly observed that there a good interfacial bonding between Al_2O_3/SiC and polymer material matrix. Hence, no voids, broken particles and plastic deformation are found on the surface of the PA6. However, the surface morphology of specimen-3 composites is formed to display a very smooth pattern of PA6. The enhanced composite performance is due to improve interfacial relations between the PA6/SiC/Al_2O_3 particles. In summary, the uniform distribution of the Al_2O_3/SiC particles in the microstructure of the PA6 material is the major responsible factor for the improvement in the mechanical properties.

3.3 Fourier Transform Infra-Red (FT-IR) Spectroscopy Method

FT-IR spectroscopy is one of the most important tools for both qualitative and quantitative characterization of organic materials, and in particular, polymers. FT-IR spectroscopy is based on the interaction of infrared light with molecules. The energy absorptivity of chemical bonds creates their FT-IR spectrum. To understand the relations between structure and properties of the composites containing SiC, Al_2O_3 and polymer PA6 matrix, FT-IR

spectroscopy is conducted on Shimadzu (8400S Model) machine with a maximum resolution of 0.85 cm^{-1}.

Figure 12a indicates that the main characteristic bands of doped PA6, alumina and SiC appear in FT-IR spectrum (specimen-2). It is observed that the peak at the wave number 572.48 cm^{-1} shows the presence of the C–Br whereas the peak at 679.96 cm^{-1} shows the presence of C–Cl (alkyl halide). The peak at 1014.66 and 1629.66 cm^{-1} represents the presence of C–F and C=C respectively. The peak attained in the spectrum at 2851.86 and 2919.42 cm^{-1} proves the presence of C–H stretch bonding. Figure 12b signifies that the main characteristic bands of doped PA6, alumina and SiC appear in FT-IR spectrum (specimen-3). From the figure, it is observed that the peak at the wave number 592.12 cm^{-1} shows the presence of the C–Br whereas the peak at 1043.96 shows the presence of C–F (alkyl halide). The peak at 2330.42 and 3022.25 cm^{-1} denotes the presence of C–H and O–H respectively. The peak attained in the spectrum at 3747.54 and 3908.48 cm^{-1} proves the presence of O–H stretch free bonding.

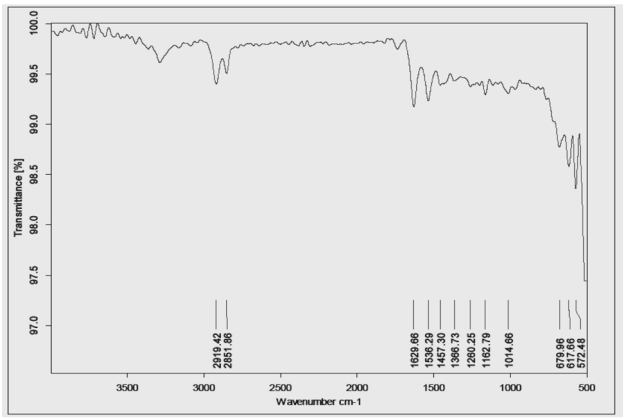

(a) Specimen-2

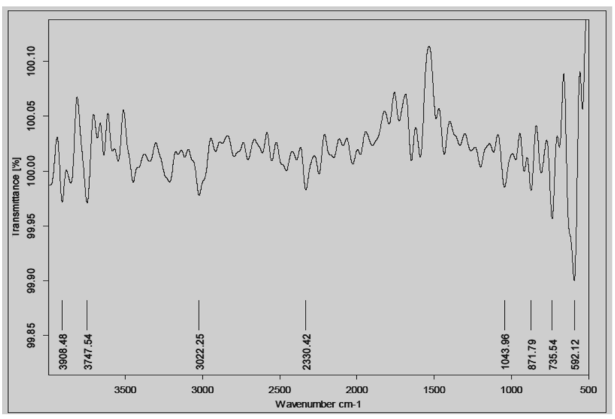

(b) Specimen - 3

Fig. 12 FT-IR Spectroscopy of PA6 hybrid composite specimen

3.4 Thermogravimetric Analysis (TGA)

TGA measures the loss of weight in material as a function of temperatures (or time) under controlled atmosphere to determine the thermal stability and composition. The thermal decomposition studies were performed over a temperature range of 50–600 °C using an EXSTAR TG/DTA 6300, Hitachi, Japan under both nitrogen and air environments at the temperature between of 27 and 700 °C/min. The heating rate was maintained at 10 °C. The temperature and the weight scales were calibrated using high-purity standards (Nickel and Iron) over a specific range of heating rates with a calibration parameter of their respective Curie points.

Thermal degradation profiles of the optimally reinforced specimen-2 (Al_2O_3—5 % and SiC—10 %) composites were determined from the TG and DTA thermogram as represented in Fig. 13. As expected the two stages of degradation are evident in both the profiles which corresponded to temperature regions for different constituents like moisture evaporation (upto 100 °C) and degradation of the material of Al_2O_3 and SiC (200–500 °C).The depolymerization of Al_2O_3 and SiC usually occurs between 400 and 500 °C. The initial peak at 98 °C in raw for the Al_2O_3 and SiC data obviously represent the loss of moisture and other volatiles at the first degradation which is observed between room temperature and 100 °C. Further, the next peak which was seen around 460 °C denotes differential thermal analysis (DTA) degradation of Al_2O_3 and SiC are prominent peak appears at the temperature corresponding to the maximum degradation rate. Moreover, optimal Al_2O_3 and SiC reinforced with PA6 composites increases the degradation temperature (400–600 °C) which is due to retention and improvement of the structural order and reduction in the amorphous content. A greater crystalline structure essentially requires a higher degradation temperature which is clearly evident in optimal Al_2O_3 and SiC with PA6 composites. The derivative thermogravimetric (DTG) curve displays the decomposition temperature of Al_2O_3 and SiC composite material value of above 420 °C.

Thermal degradation profiles of the optimally reinforced specimen-3 (PA6—85 %, Al_2O_3—10 % and SiC—5 %) composites were determined from the TG and DTA thermogram as represented in Fig. 14. As expected the two stages of degradation are evident in both the profiles which corresponded to temperature regions for different constituents like moisture evaporation (upto 100 °C) and degradation of the material of Al_2O_3 and SiC (250–500 °C). The depolymerization of Al_2O_3 and SiC usually occurs between 450 and 500 °C, The initial peak at 95 °C in raw for the Al_2O_3 and SiC data obviously represent the loss of moisture and other volatiles at the first degradation which is observed between room temperature and 100 °C.

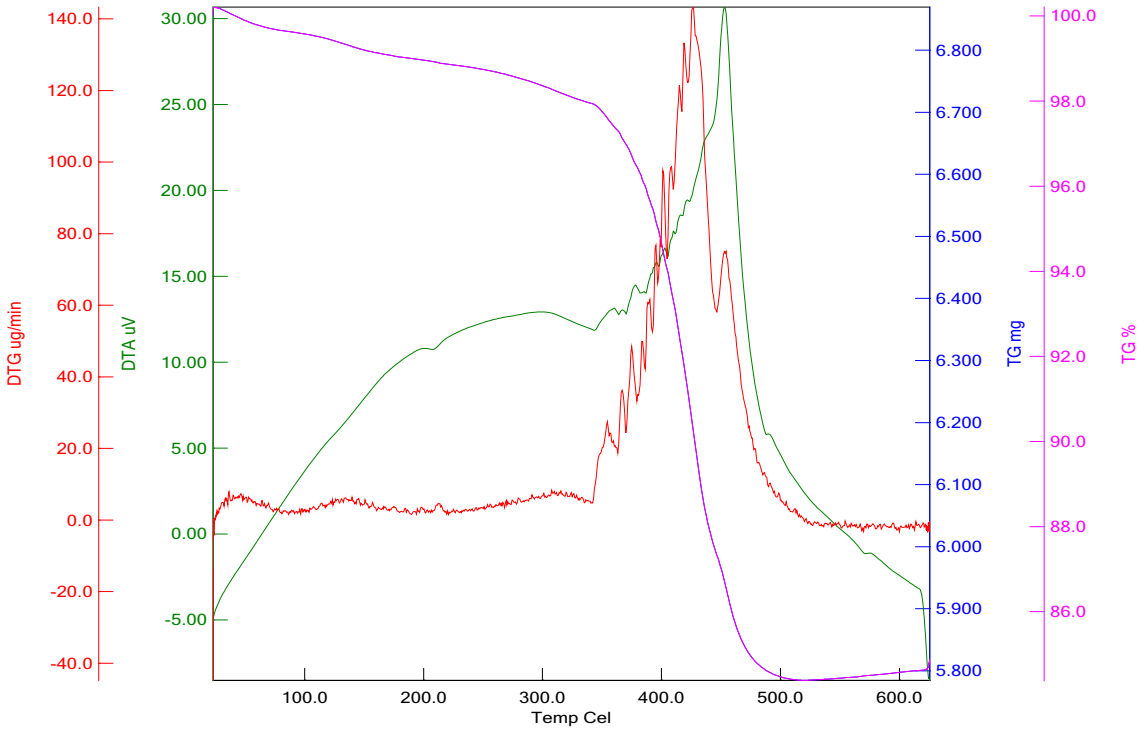

Fig. 13 TGA thermogram of specimen-2

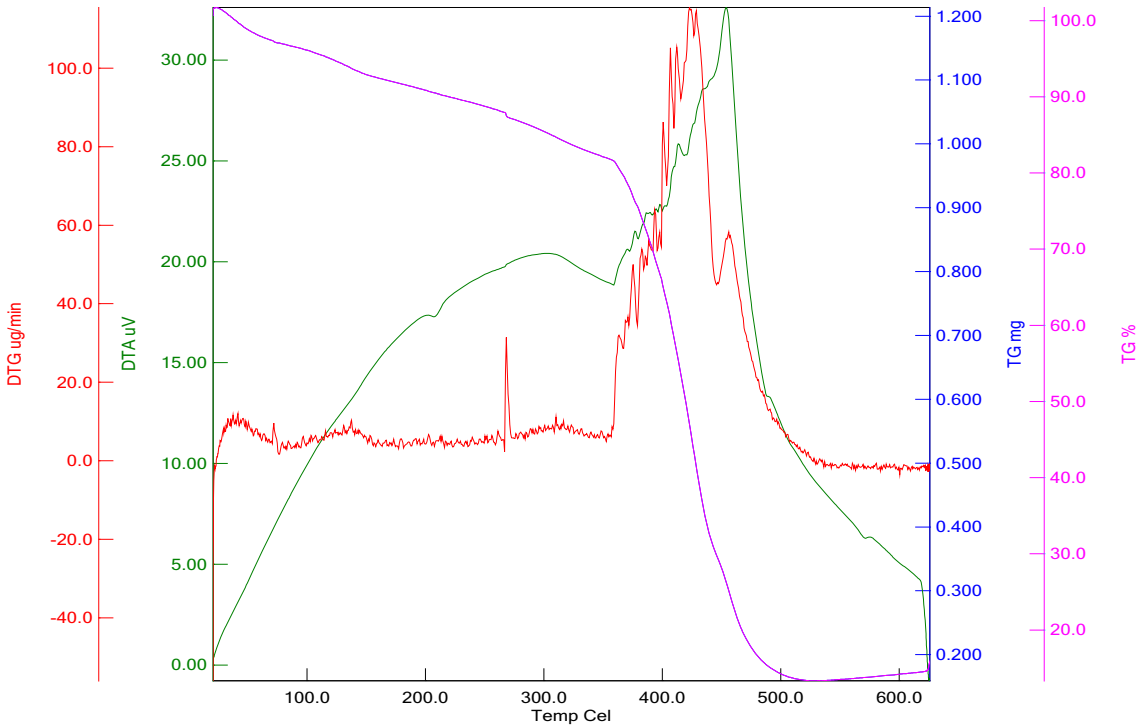

Fig. 14 TGA thermogram of specimen-3

Further, the next peak which was seen around 465 °C denotes DTA degradation of Al_2O_3 and SiC prominent peak appears at the temperature corresponding to the maximum degradation rate. Moreover, optimal Al_2O_3 and SiC composites increase the degradation temperature (450–600 °C) which is due to retention and improvement of the

structural order and reduction in the amorphous content. A greater crystalline structure essentially requires a higher degradation temperature which is clearly evident in optimal Al_2O_3 and SiC reinforced with PA6 composites. The DTG curve displays the decomposition temperature of Al_2O_3 and SiC composite material value of above 430 °C.

4 Conclusion

The PA6-based hybrid composites simultaneously reinforced with Al_2O_3 and SiC were successfully prepared using injection moulding machine. The influence of different weight percentages of Al_2O_3 and SiC on the mechanical properties of PA6 composites was experimentally investigated. The following conclusions are drawn from the present research study:

(a) The mechanical behavior test results show that addition of Al_2O_3 and SiC particles content had an obvious effect on reinforcing the PA6 matrix. Moreover, by introducing 10 wt% of Al_2O_3 and 5 wt% of SiC exhibit improved mechanical properties such as tensile strength, flexural strength, impact strength and hardness.

(b) The uniform distribution and incorporation of the Al_2O_3 and SiC particles in the microstructure of the PA6 material is the major factor responsible for the enhancement of the mechanical properties. SEM observation confirms the stronger interfacial bonding characteristics of PA6 composites.

(c) Moreover, TGA showed that the incorporation of Al_2O_3 and SiC could improve the thermal characteristics of the PA6 composites.

(d) Our findings are useful for providing some practical guidance for the preparation of composites with good mechanical and thermal characteristics.

References

1. Y. Wang, K.S. Chen, J. Mishler, S.C. Cho, X.C. Adroher, Appl. Energy **88**(4), 981–1007 (2011)
2. P. Latko, A. Boczkowska, *In Flexible and Stretchable Electronic Composites* (Springer, Berlin, 2016), pp. 135–160
3. S. Bahadur, D. Tabor, Polym. Wear Control **287**, 253–268 (1985)
4. K. Song, Y. Zhang, J. Meng, E.C. Green, N. Tajaddod, H. Li, M. L. Minus, Materials **6**, 2543–2577 (2013)
5. M. Palabiyik, S. Bahadur, Wear **246**, 149–158 (2000)
6. S. Bose, P.A. Mahanwar, J. Miner. Mater. Charact. Eng. **3**, 23 (2004)
7. J. Shi, Y. Wang, Y. Gao, H. Bai, Compos. Sci. Technol. **68**, 1338–1347 (2008)
8. F. Ularych, M. Sova, J. Vokrouhlecký, B. Turcic, Polym. Compos. **14**, 229–237 (1993)
9. G. Tang, D. Chang, D. Wang, J. He, W. Mi, J. Zhang, W. Wang, Polym. Plast. Technol. Eng. **51**, 377–380 (2012)
10. H. Unal, Mater. Des. **25**, 483–487 (2004)
11. Y. Zhang, S. Li, J. Han, Y. Zhou, Ceram. Int. **38**, 1261–1266 (2012)
12. M.R. Zakaria, H.M. Akil, M.H.A. Kudus, S.S.M. Saleh, Compos. A. Appl. Sci. Manuf. **66**, 109–116 (2014)
13. L. Meszaros, T. Deák, G. Balogh, T. Czvikovszky, T. Czigány, Compos. Sci. Technol. **75**, 22–27 (2013)
14. B.P. Chang, H.M. Akil, R.M. Nasir, Procedia. Eng. **68**, 88–94 (2013)
15. A. Nassar, E. Nassar, Nanosci. Nanoeng. **1**, 89–93 (2013)
16. S. Sathees Kumar, G. Kanagaraj, Int. J. Adv. Eng. Technol. **7**, 69–74 (2016)
17. S. Sathees Kumar, G. Kanagaraj, Int. J. Polym. Anal. Charact. (2016). doi:10.1080/1023666X.2016.1160671
18. J.F. Sharkelford, Y.H. Han, S. Kim, S.H. Kwon, *CRC Materials Science Engineering Handbook*, 4th edn. (CRC Press, Boca Raton, 2015), p. 473
19. C. Barnes, P. Shrotriya, P. Molian, Int. J. Mach. Tools. Manuf. **47**, 1864–1874 (2007)
20. L. Kumari, T. Zhang, G.H. Du, W.Z. Li, Q.W. Wang, A. Datye, Compos. Sci. Technol. **68**, 2178–2183 (2008)
21. S. Kalpakjian, S.R. Schmid, *Manufacturing Processes for Engineering Materials, Pearson Education*, 4th edn. (Prentice-Hall, New Delhi, 2002), p. 560